



Article

Guangyuanite, $\text{Pb}_3\text{Cl}_3(\text{Se}^{4+}\text{O}_3)(\text{OH})$, a new lead chloride selenite mineral from the El Dragón mine, Potosí, Bolivia

Hexiong Yang¹ , Xiangping Gu² , James A. McGlasson¹, Ronald B. Gibbs¹ and Robert T. Downs¹

¹Department of Geosciences, University of Arizona, 1040 E. 4th Street, Tucson, AZ 85721-0077, USA; and ²School of Geosciences and Info-Physics, Central South University, Changsha, Hunan 410083, China

Abstract

A new mineral species, guangyuanite, ideally $\text{Pb}_3\text{Cl}_3(\text{Se}^{4+}\text{O}_3)(\text{OH})$, was discovered from the El Dragón mine, Antonio Quijarro Province, Potosí Department, Bolivia. It occurs as equant crystals. Associated minerals are Co-bearing krut'aite–penroseite, chalcomenite, schmierderite, olsacherite, phosgenite, anglesite, cerussite and franksousaite. Guangyuanite is pale yellow–brown in transmitted light, transparent with white streak and vitreous lustre. It is brittle and has a Mohs hardness of ~3. No parting or cleavage was observed. The calculated density is 7.63 g/cm³. An electron microprobe analysis yielded an empirical formula [based on 7 (O + Cl) atoms per formula unit] of $\text{Pb}_{3.02}\text{Cl}_{3.01}(\text{Se}_{0.99}^{4+}\text{O}_3)(\text{OH})$, which can be simplified to $\text{Pb}_3\text{Cl}_3(\text{Se}^{4+}\text{O}_3)(\text{OH})$.

Guangyuanite is isostructural with synthetic $\text{Pb}_3\text{Br}_3(\text{Se}^{4+}\text{O}_3)(\text{OH})$. It is orthorhombic, with space group *Pnma* and unit-cell parameters $a = 11.0003(5)$, $b = 10.6460(5)$, $c = 7.7902 \text{ \AA}$, $V = 912.31(6) \text{ \AA}^3$ and $Z = 4$. The crystal structure of guangyuanite contains two symmetrically-distinct Pb (Pb1 and Pb2) cations, with Pb1 coordinated by eight anions (4O + 4Cl) and Pb2 only by six anions (3O + 3Cl), forming a marked lopsided coordination typical of Pb^{2+} with a stereochemically active $6s^2$ lone electron pair. The Se^{4+} cation forms a typical $[\text{Se}^{4+}\text{O}_3]$ trigonal pyramid. The crystal structure of guangyuanite can be described as consisting of layers of edge-sharing $[\text{Pb}_1\text{O}_4\text{Cl}_4]$ polyhedra parallel to (100). These layers are linked together by sharing polyhedral corners (Cl atoms), as well as $[\text{Pb}_2\text{O}_3\text{Cl}_3]$ and $[\text{Se}^{4+}\text{O}_3]$ groups. Chemically, guangyuanite is one of six lead chloride selenite minerals reported thus far and closely related to orlandiite $\text{Pb}_3\text{Cl}_4(\text{Se}^{4+}\text{O}_3)\cdot\text{H}_2\text{O}$.

Keywords: guangyuanite; lead selenite chloride; new mineral; crystal structure; Raman; El Dragón mine; Bolivia

(Received 19 August 2023; accepted 28 November 2023; Accepted Manuscript published online: 7 December 2023; Associate Editor: David Hibbs)

Introduction

Guangyuanite, ideally $\text{Pb}_3\text{Cl}_3(\text{Se}^{4+}\text{O}_3)(\text{OH})$, is a new mineral species discovered from the El Dragón mine, Antonio Quijarro Province, Potosí Department, Bolivia. It is named in honour of the late Chinese mineralogist, Prof. Chen Guangyuan (1920–1999). Prof. Chen obtained his Degree of Licentiate from the Uppsala University of Sweden in 1951 and became a teacher and researcher at Peking University between 1951 and 1952 and later at the China University of Geosciences in Beijing from 1952 to 1999. Prof. Chen is regarded as the pioneer and leader for both teaching and research in genetic and exploration mineralogy in China from the 1950's to 1980's. He made significant contributions to the systematic studies of the genesis of minerals, especially on genetic classification of mineral groups, typomorphic mineralogy, and mineralogical mapping for exploration, with over 100 publications and 9 books, including the well-recognised “*Genetic Mineralogy and Prospecting Mineralogy*”, which has been adopted by many universities in China. The new mineral and its name (symbol Gyn) have been approved by the

Commission on New Minerals, Nomenclature and Classification (CNMNC) of the International Mineralogical Association (IMA 2022-124, Yang *et al.*, 2023d). The co-type samples have been deposited at the University of Arizona Alfie Norville Gem and Mineral Museum (Catalogue # 22714) and the RRUFF Project (deposition # R210013) (<http://rruff.info>) (Lafuente *et al.*, 2015).

Lead chloride selenite minerals are rather rare in Nature and only six minerals contain $\text{Pb–Cl–}(\text{Se}^{4+}\text{O}_3)^{2-}$ in the current IMA-approved mineral list (Table 1). Interestingly, all of these minerals have only been described in the past 25 years. Nevertheless, synthetic lead chloride selenite materials have been an attractive subject in numerous investigations. On the one hand, selenite materials can form a diversity of unusual structures due to the presence of the stereochemically active lone-pair electrons in Se^{4+} , which can serve as structure-directing agents (Berdonosov *et al.*, 2000, 2012; Wickleder, 2002 and references therein). The lone-pair electrons in Se^{4+} are not involved in the formation of chemical bonds, thus acting like terminal ligands and resulting in various voids in the structure. Furthermore, the asymmetric coordination of $(\text{Se}^{4+}\text{O}_3)^{2-}$ (trigonal pyramid) may also give rise to noncentrosymmetric structures with interesting physical properties, such as nonlinear optical second-harmonic generation, piezoelectric, ferroelectric and pyroelectric properties (Porter *et al.*, 2001; Ok *et al.*, 2001; Ok and Halasyamani, 2002;

Corresponding author: Hexiong Yang; Email: hyang@arizona.edu

Cite this article: Yang H., Gu X., McGlasson J.A., Gibbs R.B. and Downs R.T. (2024) Guangyuanite, $\text{Pb}_3\text{Cl}_3(\text{Se}^{4+}\text{O}_3)(\text{OH})$, a new lead chloride selenite mineral from the El Dragón mine, Potosí, Bolivia. *Mineralogical Magazine* 88, 97–104. <https://doi.org/10.1180/mgm.2023.93>

Table 1. List of lead-selenite-chloride minerals.

Mineral	Ideal chemical formula	Symmetry	Ref.
Allochalcocelinite	$\text{Cu}^{1+}\text{Cu}_5^{2+}\text{PbO}_2(\text{SeO}_3)_2\text{Cl}_5$	$C2/m$	(1)
Guangyuanite	$\text{Pb}_3\text{Cl}_3(\text{Se}^{4+}\text{O}_3)(\text{OH})$	$Pnma$	(2)
Orlandiite	$\text{Pb}_3\text{Cl}_4(\text{Se}^{4+}\text{O}_3)\cdot\text{H}_2\text{O}$	$P\bar{1}$	(3)
Prewittite	$\text{KPb}_{1.5}\text{ZnCu}_6\text{O}_2(\text{SeO}_3)_2\text{Cl}_{10}$	$Pnmm$	(4)
Sarrabusite	$\text{Pb}_5\text{CuCl}_4(\text{SeO}_3)_4$	$C2/c$	(5)
Wangukuirenite	$\text{Pb}_3\text{Cl}_2(\text{SeO}_3)_2$	$C2/c$	(6,7)

References: (1) Vergasova *et al.* (2005); (2) This study; (3) Demartin *et al.* (2003); (4) Shuvalov *et al.* (2013); (5) Gemmi *et al.* (2012); (6) Porter *et al.* (2001); (7) Yang *et al.* (2023a).

Kong *et al.*, 2006; Kim *et al.*, 2009, 2010). Conceivably, introduction of other cations with lone-pair electrons into selenite materials (such as Tl^+ , Sn^{2+} , Pb^{2+} , Sb^{3+} and Bi^{3+}) will offer more new phases from which additional functionalities may arise (Ok *et al.*, 2001; Porter *et al.*, 2001; Dityatyev *et al.* 2004; Krivovichev *et al.*, 2004; Kim *et al.* 2009; Zhang *et al.*, 2012). On the other hand, because both Se^{4+} and X^- ($\text{X} = \text{Cl}, \text{Br}$ and I) can act as ‘chemical scissors’ (Johnsson *et al.*, 2000, 2003; Millet *et al.*, 2001), considerable effort has also been made to incorporate X^- anions into selenite materials to obtain low dimensional structures, which has resulted in a number of compounds with fascinating magnetic properties (e.g. Becker *et al.*, 2006, 2007; Jiang and Mao, 2006; Zhang *et al.*, 2009, 2010, 2012). Thus far, at least 10 different lead halide selenite phases have been synthesised and structurally characterised, including $\text{Pb}_3(\text{SeO}_3)(\text{SeO}_2\text{OH})\text{Cl}_3$ (Porter *et al.*, 2001), $\text{Pb}_3(\text{SeO}_3)_2\text{Cl}_2$, $\text{Pb}_3(\text{SeO}_3)_2\text{Br}_2$, $\text{Pb}_3(\text{SeO}_3)_2\text{I}_2$, $\text{Pb}_2\text{Cd}_3(\text{SeO}_3)_4\text{I}_2(\text{H}_2\text{O})$ (Porter and Halasyamani, 2001; Berdonosov *et al.* 2012; Zhang *et al.*, 2012), $(\text{Pb}_2\text{Cu}_9^{2+}\text{O}_4)(\text{SeO}_3)_4(\text{Cu}^+\text{Cl}_2)\text{Cl}_5$, $(\text{PbCu}_5^{2+}\text{O}_2)(\text{SeO}_3)_2(\text{Cu}^+\text{Cl}_2)\text{Cl}_3$, and $(\text{Pb}_x\text{Cu}_{6-x}^{2+}\text{O}_2)(\text{SeO}_3)_2(\text{Cu}^+\text{Cl}_2)\text{K}_{(1-x)}\text{Cl}_{(4-x)}$ ($x = 0.20$) (Kovrugin *et al.*, 2015), $(\text{Cu}^{2+}\text{Pb}_6(\text{SeO}_3)_4\text{Br}_6$, $\text{Cu}^{2+}\text{Pb}_2(\text{SeO}_3)_2\text{Br}_2$, $\text{Cu}_3^{2+}\text{Pb}_{2.4}(\text{SeO}_3)_5\text{Br}_{0.8}$, $\text{Cu}_2^{2+}\text{Pb}(\text{SeO}_3)_2\text{Br}_2$, $\text{Cu}_4^{2+}\text{Pb}(\text{SeO}_3)_4\text{Br}_2$, $[\text{Cu}_9^{2+}\text{Pb}_2\text{O}_4](\text{Cu}^+\text{Br}_2)(\text{SeO}_3)_4\text{Br}_5$, $[\text{Cu}_7^{2+}\text{PbO}_3](\text{Cu}^+\text{Br})_{0.35}(\text{SeO}_3)_3\text{Br}_4$, $[\text{Cu}_8^{2+}\text{Pb}_2\text{O}_4](\text{Cu}^+\text{Br})_{1.5}(\text{SeO}_3)_4\text{Br}_4$, $[\text{Cu}_6^{2+}\text{Pb}_3\text{O}_4](\text{Cu}^+\text{Pb}_{1.27}\text{Br}_{3.54})(\text{SeO}_3)_4\text{Br}_2$) (Siidra *et al.*, 2018), $\text{Pb}_2\text{Cd}(\text{SeO}_3)_2\text{X}_2$ (Gong *et al.* 2019), $\text{Pb}_3(\text{SeO}_3)(\text{HSeO}_3)\text{Br}_3$, $\text{Pb}_3(\text{SeO}_3)(\text{OH})\text{Br}_3$ and $\text{CdPb}_8(\text{SeO}_3)_4\text{Cl}_4\text{Br}_6$ (Shang and Halasyamani, 2020). In all these compounds, Se^{4+} only forms bonds with O atoms, whereas Pb^{2+} can form bonds with both X and O atoms. This paper describes the physical and chemical properties of guangyuanite, and its crystal structure determined from single-crystal X-ray diffraction data.

Sample description and experimental methods

Occurrence, physical and chemical properties, and Raman spectra

Guangyuanite was found on a specimen (Fig. 1) collected from the El Dragón mine (19°49′15″S, 65°55′0″W), Antonio Quijarro Province, Potosí Department, Bolivia. Associated minerals are Co-bearing krut’aite–penroseite, chalcocite, schmiederite, olsacherite, phosgenite, anglesite, cerussite and franksousaite. Detailed descriptions on the geology and mineralogy of the El Dragón mine were given by Grundmann *et al.* (1990, 2007) and Grundmann and Förster (2017). This is an epithermal deposit consisting of a single selenide vein hosted by sandstones and shales. The major ore mineral is krut’aite, CuSe_2 , varying in composition to penroseite, NiSe_2 . Later solutions rich in Bi, Pb and Hg resulted in the crystallisation of minerals such as clausenthalite, petrovicite, watkinsonite and the recently described minerals eldragónite, $\text{Cu}_6\text{BiSe}_4(\text{Se}_2)$ (Paar *et al.*, 2012), grundmannite,



Figure 1. The specimen on which the new mineral guangyuanite, indicated by the blue arrow, was found. Specimen R210013.

CuBiSe_2 (Förster *et al.*, 2016), hansblockite, $(\text{Cu,Hg})(\text{Bi,Pb})\text{Se}_2$ (Förster *et al.*, 2017), cerromonjonte, CuPbBiSe_3 (Förster *et al.*, 2018) and nickeltyrrellite, CuNi_2Se_4 (Förster *et al.*, 2019). Oxidation produced a wide range of secondary Se-bearing minerals, such as favreuite, $\text{PbBiCu}_6\text{O}_4(\text{SeO}_3)_4(\text{OH})\cdot\text{H}_2\text{O}$ (Mills *et al.*, 2014), alfredopetrovite, $\text{Al}_2(\text{Se}^{4+}\text{O}_3)_3\cdot 6\text{H}_2\text{O}$ (Kampf *et al.*, 2016b), franksousaite, $\text{PbCu}(\text{Se}^{6+}\text{O}_4)(\text{OH})_2$ (Yang *et al.*, 2022), bernard-evansite, $\text{Al}_2(\text{Se}^{4+}\text{O}_3)_3\cdot 6\text{H}_2\text{O}$ (Yang *et al.*, 2023b), petermegawite, $\text{Al}_6(\text{Se}^{4+}\text{O}_3)_3[\text{SiO}_3(\text{OH})](\text{OH})_9\cdot 10\text{H}_2\text{O}$ (Yang *et al.*, 2023c) and the new mineral guangyuanite, described herein.

Guangyuanite occurs as equant brown-yellowish crystals (Fig. 2) in a vug, where only two crystals were found. The matrix consists of Co-bearing krut’aite–penroseite. Individual crystals of guangyuanite are up to $0.40 \times 0.30 \times 0.30$ mm. Guangyuanite is pale yellow–brown in transmitted light, transparent with white streak and vitreous lustre. It is brittle and has a Mohs hardness of ~ 3 . No cleavage was observed. The density could not be measured because it is greater than available high-density liquids and there is insufficient material for the direct measurement. The calculated density is 6.73 g/cm^3 on the basis of the empirical chemical formula and unit cell volume from single-crystal X-ray

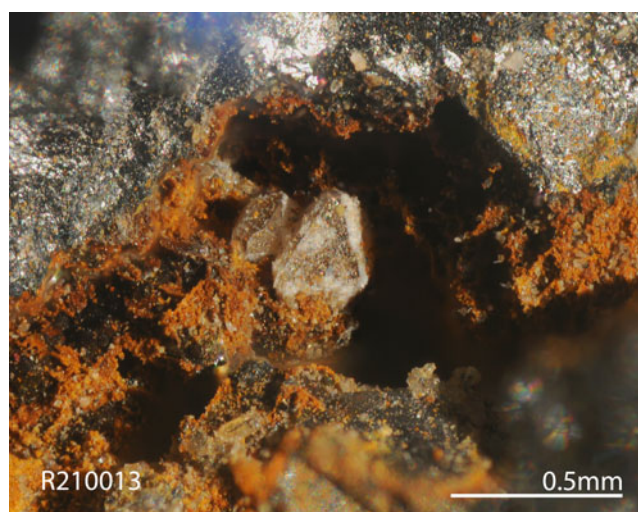


Figure 2. A microscopic view of two yellow-brown guangyuanite crystals in a vug, specimen R210013.

Table 2. Chemical data (in wt.%) for guangyuanite.

Constituent	Mean	Range	S.D.	Probe standard
PbO	76.90	75.35–77.87	0.94	Pb(SO ₄) (synthetic)
SeO ₂	12.49	11.46–13.75	0.89	PbSe (synthetic)
Cl	12.18	12.04–12.60	0.21	PbCl ₂ (synthetic)
O≡Cl	–2.75	–(2.72–2.84)	0.05	
H ₂ O _{calc}	1.03			Added in ideal value
Total	99.85			

diffraction data. No optical data were measured because the indices of refraction are too high for measurement with available index liquids. The calculated average index of refraction is 2.04 for the empirical formula based on the Gladstone-Dale relationship (Mandarino, 1981). Guangyuanite is insoluble in water and hydrochloric acid.

The chemical composition was determined using a Shimadzu-1720 electron microprobe (WDS mode, 15 kV, 10 nA, and a beam diameter of 2 μm). The standards used for the probe analysis are given in Table 2, along with the determined compositions (6 analysis points). The resultant chemical formula, calculated on the basis of 7 (O,Cl) atoms per formula unit (from the structure determination), is Pb_{3.02}Cl₃(Se_{0.99}O₃)(OH), which can be simplified to Pb₃Cl₃(Se⁴⁺O₃)(OH). The ideal formula requires (wt.%) PbO 76.80, SeO₂ 12.73, H₂O 1.03, Cl 12.20, O ≡ Cl –2.76, total 100 wt.%.

The Raman spectrum of guangyuanite (Fig. 3) was collected on a randomly oriented crystal with a Thermo Almega microRaman system, using a solid-state laser with a wavelength of 532 nm at 50% of 150 mW power and a thermoelectric cooled CCD detector. The laser is partially polarised with 4 cm^{–1} resolution and a spot size of 1 μm.

X-ray crystallography

Both the powder and single-crystal X-ray diffraction data for guangyuanite were collected on a Rigaku Xtalab Synergy D/S 4-circle diffractometer. Powder X-ray diffraction data were

collected with CuKα radiation in the Gandolfi powder mode at 50 kV and 1 mA (Table 3) and the unit-cell parameters were refined using the program by Holland and Redfern (1997): $a = 10.9920(6)$, $b = 10.6387(7)$, $c = 7.7863(5)$ Å, and $V = 910.55(6)$ Å³.

Single-crystal X-ray diffraction data of guangyuanite were collected with MoKα radiation from a 0.05 × 0.05 × 0.04 mm fragment. The systematic absences of reflections suggest possible space group $Pn2_1a$ or $Pnma$. The structure was solved and refined using SHELX2019 (Sheldrick, 2015a, 2015b) based on space group $Pnma$, because it produced better refinement statistics in terms of bond lengths and angles, atomic displacement parameters, and R factors. The H atom was located through difference-Fourier syntheses. The positions of all atoms were refined with anisotropic displacement parameters, except for the H atom, which was refined with the U_{iso} set to 1.5 times that of O3 on which it rides. The refinement statistics are given in Table 4. Final atomic coordinates and displacement parameters are given in Tables 5 and 6, respectively. Selected bond lengths are presented in Table 7. The bond valences were calculated using the parameters given by Brown (2009) (Table 8). The crystallographic information file has been deposited with the Principal Editor of *Mineralogical Magazine* and is available as Supplementary material (see below).

Crystal structure description and discussion

Guangyuanite is isotypic with synthetic Pb₃Br₃(Se⁴⁺O₃)(OH) (Shang and Halasyamani, 2020). Its structure contains two symmetrically distinct Pb (Pb1 and Pb2), two Cl (Cl1 and Cl2), one Se, one H and three O (O1, O2 and O3) atoms, among which O3 is hydroxyl (OH) (Table 8) and forms the hydrogen bond with O2 (Table 7). The Pb1 cation is in a polyhedron coordinated by 4O and 4Cl atoms (Fig. 4a), whereas the Pb2 cation is only bonded by six anions (3O + 3Cl) (Fig. 4b), forming a marked one-sided coordination typical of Pb²⁺ with a stereochemically-active 6s² lone-electron pair. The Se⁴⁺ cation is bonded to three O atoms, giving rise to the typical [Se⁴⁺O₃] trigonal pyramid.

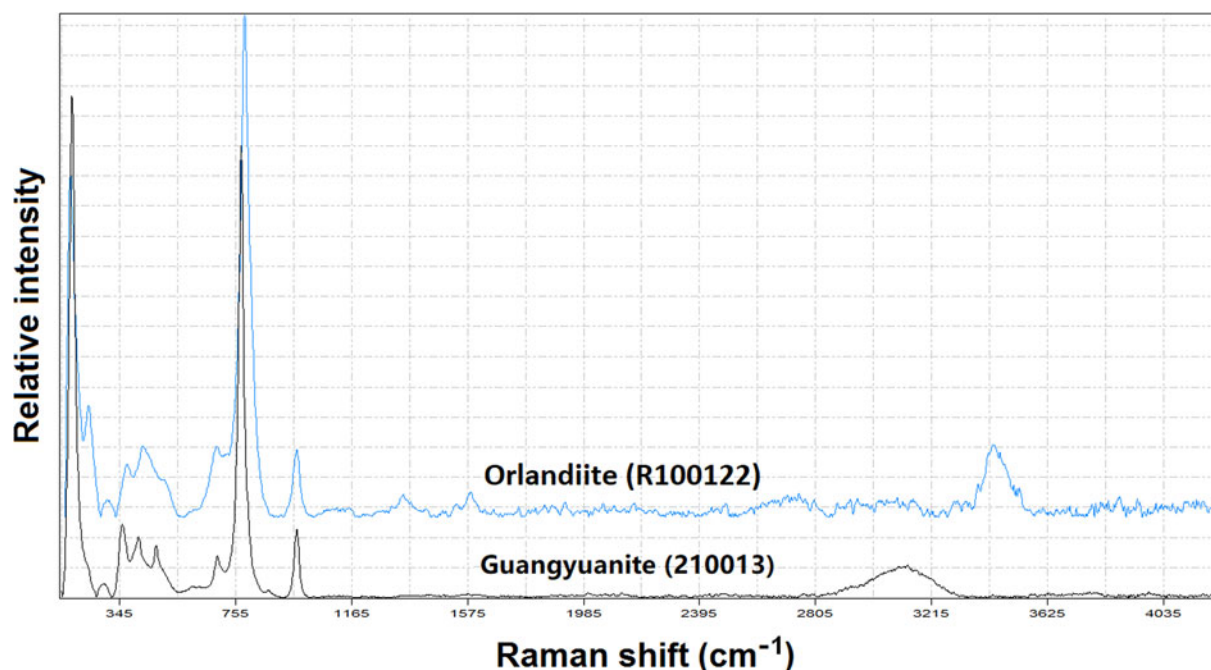
**Figure 3.** Raman spectra of guangyuanite (R210013) and orlandiite (R100122).

Table 3. Powder X-ray diffraction data (d in Å, I in %) for guanyuanite.

l_{cal}	l_{meas}	d_{meas}	d_{calc}	hkl	l_{cal}	l_{meas}	d_{meas}	d_{calc}	hkl	l_{cal}	l_{meas}	d_{meas}	d_{calc}	hkl
15.0	18.4	6.374	6.357	1 0 1	45.2	42.3	2.593	2.593	4 0 1	6.8	11.1	1.632	1.631	2 3 4
6.1	21.5	6.320	6.287	0 1 1	51.6	70.6	2.523	2.523	0 1 3	3.8	3.0	1.597	1.598	1 6 2
47.3	63.7	5.489	5.458	1 1 1	14.0	16.2	2.427	2.423	3 3 1	3.6	4.7	1.568	1.565	3 6 1
13.9	17.2	4.897	4.887	2 1 0	18.0	23.2	2.388	2.387	3 2 2	14.6	19.3	1.542	1.545	4 5 2
21.8	20.3	4.507	4.493	2 0 1	11.7	16.5	2.347	2.348	2 0 3	3.4	3.5	1.521	1.523	4 2 4
67.4	62.1	4.150	4.140	2 1 1	2.1	1.2	2.245	2.247	4 0 2	14.7	21.1	1.497	1.498	6 0 3
21.6	10.8	4.093	4.081	1 2 1	19.6	39.4	2.197	2.198	4 1 2	5.5	6.9	1.478	1.480	7 2 1
8.3	31.7	3.901	3.895	0 0 2	48.0	32.0	2.173	2.174	4 3 0	8.9	2.5	1.462	1.464	4 6 1
47.3	21.7	3.833	3.825	2 2 0	10.1	9.2	2.134	2.133	3 3 2	2.8	6.4	1.446	1.444	7 1 2
7.9	13.1	3.679	3.672	1 0 2	18.6	26.5	2.092	2.094	4 3 1	8.3	6.7	1.424	1.427	0 3 5
6.9	11.0	3.485	3.471	1 1 2	6.2	12.0	2.061	2.054	0 5 1	2.1	6.2	1.412	1.416	2 6 3
22.7	24.0	3.435	3.433	2 2 1	3.5	9.2	1.981	1.986	2 5 0	8.0	11.9	1.386	1.389	6 5 0
9.1	6.2	3.337	3.318	3 0 1	41.3	47.9	1.957	1.958	2 3 3	5.0	11.1	1.381	1.381	2 3 5
100.0	84.5	3.235	3.229	0 3 1	26.4	18.4	1.922	1.924	2 5 1	5.6	10.2	1.349	1.354	8 0 1
31.9	83.1	3.178	3.167	3 1 1	3.4	6.2	1.888	1.885	5 1 2	3.0	4.2	1.332	1.338	3 5 4
58.7	100.0	3.149	3.143	0 2 2	5.9	2.5	1.857	1.859	4 1 3	2.6	2.7	1.309	1.309	6 5 2
16.0	12.7	3.105	3.099	1 3 1	17.3	20.8	1.832	1.836	2 0 4	3.8	6.2	1.298	1.298	0 0 6
27.7	41.2	3.023	3.022	1 2 2	11.1	14.6	1.803	1.807	6 1 0	5.9	9.6	1.273	1.276	2 6 4
19.1	36.0	2.818	2.816	3 2 1	24.5	35.0	1.775	1.779	4 2 3	6.6	9.9	1.255	1.259	0 8 2
44.2	47.9	2.787	2.785	2 3 1	2.6	2.2	1.720	1.720	3 0 4	8.0	9.5	1.247	1.249	6 3 4
36.9	44.0	2.731	2.729	2 2 2	13.5	20.6	1.688	1.692	6 2 1	3.1	9.0	1.226	1.226	2 5 5
13.7	12.8	2.663	2.662	0 4 0	20.2	19.8	1.645	1.646	0 5 3	3.3	2.0	1.214	1.218	8 3 2

Note: The strongest lines are given in bold.

Table 4. Crystallographic data and refinement statistics for guanyuanite and orlandiite.

	Guanyuanite	Br-analogue	Orlandiite
Ideal chemical formula	Pb ₃ Cl ₃ (Se ⁴⁺ O ₃)(OH)	Pb ₃ Br ₃ (Se ⁴⁺ O ₃)(OH)	Pb ₃ Cl ₄ (Se ⁴⁺ O ₃)·H ₂ O
Crystal symmetry	Orthorhombic	Orthorhombic	Triclinic
Space group	Pnma	Pnma	$P\bar{1}$
a (Å)	11.0003(5)	11.3059(12)	8.136(3)
b (Å)	10.6460(5)	10.8211(12)	8.430(6)
c (Å)	7.7902(3)	7.9802(9)	9.233(7)
α (°)	90	90	62.58(7)
β (°)	90	90	71.84(4)
γ (°)	90	90	75.13(4)
V (Å ³)	912.31(6)	976.32(19)	529.3(7)
Z	4	4	2
ρ_{cal} (g/cm ³)	6.348	6.839	5.699
2θ range for data collection (MoK α)	≤ 66.82	≤ 55.0	≤ 54
No. of reflections collected	8832	5448	2430
No. of independent reflections	1662	1173	2287
No. of reflections with $I > 2\sigma(I)$	1391	1049	1311
No. of parameters refined	61	61	128
R(int)	0.036	0.023	
Final R_1 , wR_2 factors [$I > 2\sigma(I)$]	0.021, 0.033	0.018, 0.036	0.047, 0.104
Goodness-of-fit	1.038	1.041	
Reference	This study	Shang and Halasyamani (2020)	Demartin <i>et al.</i> (2003)

Table 5. Fractional atomic coordinates and equivalent/isotropic displacement parameters (Å²) for guanyuanite.

Atom	x/a	y/b	z/c	U_{iso}^*/U_{eq}
Pb1	0.03892(2)	0.06809(2)	0.73752(2)	0.01942(5)
Pb2	0.20754(2)	1/4	0.08683(3)	0.02340(7)
Se	0.41181(5)	1/4	0.45852(7)	0.01118(11)
Cl1	0.48817(15)	1/4	0.05765(19)	0.0225(3)
Cl2	0.22967(11)	0.00905(10)	0.43308(16)	0.0266(2)
O1	0.0140(3)	0.1284(2)	0.0518(3)	0.0142(6)
O2	0.3907(4)	1/4	0.6747(5)	0.0176(8)
O3	0.1603(4)	1/4	0.7970(5)	0.0148(8)
H	0.240(3)	1/4	0.754(8)	0.022*

The crystal structure of guanyuanite can be described as consisting of layers of edge-sharing [Pb₁O₄Cl₄] polyhedra parallel to (100) (Fig. 5). These layers are linked together by sharing polyhedral corners (Cl atoms), as well as [Pb₂O₃Cl₃] and [Se⁴⁺O₃] groups (Fig. 6). The [PbO₄Cl₄] polyhedra are apparently a basic structural unit in many lead oxychlorides, as observed in nadorite, PbSbO₂Cl (Giuseppetti and Tadini, 1973), perite, PbBiO₂Cl (Gillberg, 1960), diabolite, CuPb₂Cl₂(OH)₄ (Cooper and Hawthorne, 1995), hematophanite Pb₄Fe₃³⁺O₈(Cl,OH) (Rouse, 1973) and chloroxiphite Pb₃CuO₂Cl₂(OH)₂ (Finney *et al.*, 1977; Siidra *et al.*, 2008).

According to Raman or IR spectroscopic studies on hydrous materials containing (SeO₃)²⁻ (e.g. Wickleder *et al.*, 2004; Frost *et al.*, 2006; Frost and Keeffe, 2008; Djemel *et al.*, 2013;

Table 6. Atomic displacement parameters (\AA^2) for guanyuanite.

Atom	U^{11}	U^{22}	U^{33}	U^{12}	U^{13}	U^{23}
Pb1	0.02362(10)	0.01669(9)	0.01796(8)	-0.00094(6)	0.00174(6)	-0.00351(6)
Pb2	0.01595(12)	0.03387(14)	0.02038(12)	0	-0.00700(10)	0
Se	0.0107(3)	0.0123(2)	0.0106(2)	0	-0.0020(2)	0
Cl1	0.0238(8)	0.0272(8)	0.0165(7)	0	0.0007(6)	0
Cl2	0.0193(6)	0.0229(5)	0.0377(7)	0.0002(4)	0.0037(5)	-0.0041(4)
O1	0.0167(15)	0.0111(13)	0.0147(14)	-0.0003(11)	0.0003(12)	0.0012(10)
O2	0.018(2)	0.023(2)	0.013(2)	0	0.0024(17)	0
O3	0.011(2)	0.0162(19)	0.017(2)	0	0.0029(17)	0

Table 7. Selected bond distances (\AA) and angles ($^\circ$) for guanyuanite and the Br-analogue.

	Guanyuanite	Br-analogue		Guanyuanite	Br-analogue
Pb1-O3	2.398(3)	2.416(3)	Pb2-O3	2.316(4)	2.348(5)
Pb1-O1	2.546(3)	2.512(3)	Pb2-O1 $\times 2$	2.507(3)	2.526(3)
Pb1-O2	2.622(3)	2.628(3)	Pb2-X2 $\times 2$	3.0851(11)	3.1912(7)
Pb1-O1	2.721(3)	2.769(3)	Pb2-X1	3.0953(17)	3.2032(9)
Pb1-X1	3.0577(12)	3.1817(7)	<Pb2-O>	2.766	2.831
Pb1-X2	3.0781(11)	3.1589(6)			
Pb1-X2	3.2283(12)	3.3765(6)	O3-H	0.94(2)	0.47(10)
Pb1-X2	3.3423(12)	3.4355(6)	H \cdots O2	1.77(2)	1.91(2)
<Pb1-O>	2.874	2.935	O3 \cdots O2	2.708(6)	2.842(7)
			\angle O3-H \cdots O2	180(6) $^\circ$	167(7) $^\circ$
Se-O2	1.700(4)	1.697(5)			
Se-O1	1.717(3) $\times 2$	1.727(4)			
<T-O>	1.711	1.710(4)			

Note: X = Cl and Br for guanyuanite and the Br-analogue, respectively. Data for the Br-analogue were taken from Shang and Halasyamani (2020)

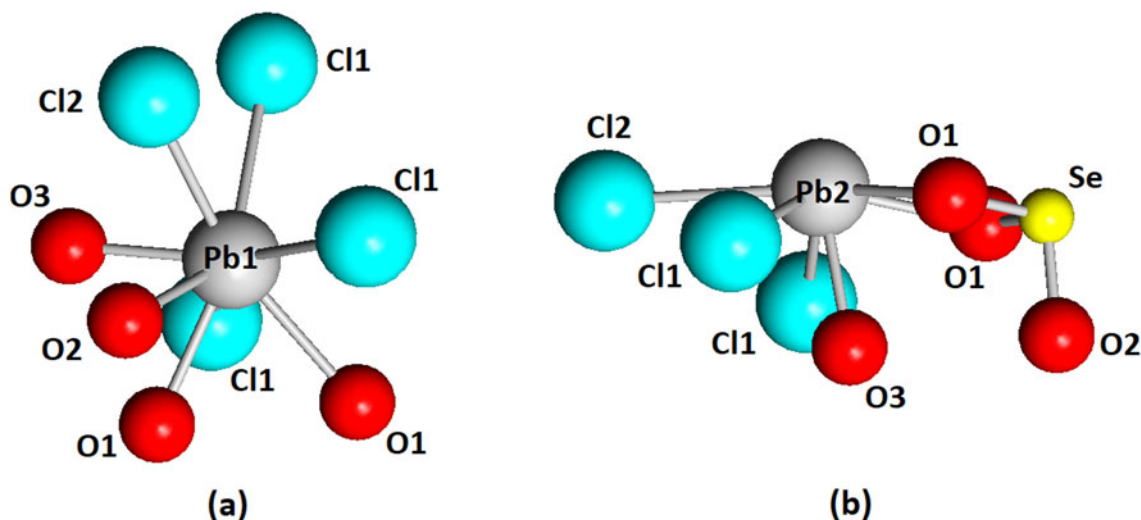
Table 8. Bond-valence sums for guanyuanite.

	Pb1	Pb2	Se	Sum
O1	0.30 0.21	0.33 $\times 2^1$	1.29 $\times 2^1$	2.14
O2	0.26 $\times 2 \rightarrow$		1.35	1.87
O3	0.41 $\times 2 \rightarrow$	0.49		1.31
Cl1	0.23 0.15 0.11	0.22 $\times 2^1$		0.71
Cl2	0.24 $\times 2 \rightarrow$	0.22		0.70
Sum	1.92	1.81	3.93	

Note: superscripts indicate the number of equivalent bonds for the respective sum arrowed.

Kasatkin *et al.*, 2014; Mills *et al.*, 2014; Kampf *et al.*, 2016a; Shang and Halasyamani, 2020), we made the following tentative assignments of major Raman bands for guanyuanite. The broad weak bands between 2850 and 3300 cm^{-1} (centred at 3130 cm^{-1}) are due to the O-H stretching modes in OH groups. The bands between 665 and 1000 cm^{-1} are ascribable to the Se^{4+} -O stretching vibrations within the Se^{4+}O_3 groups, whereas those from 320 to 570 cm^{-1} originate from the O- Se^{4+} -O bending modes. The bands below 320 cm^{-1} are associated mainly with the rotational and translational modes of Se^{4+}O_3 groups, as well as the Pb-O and Pb-Cl interactions and lattice vibrational modes.

The calculated bond-valence sums for guanyuanite (Table 8) indicate that O3 is the OH group, which forms a hydrogen bond

**Figure 4.** Atomic coordinations in guanyuanite: (a) for $[\text{Pb}_{10}\text{Cl}_4]$ polyhedron and (b) for $[\text{Pb}_2\text{O}_3\text{Cl}_3]$ and $[\text{Se}^{4+}\text{O}_3]$ groups.

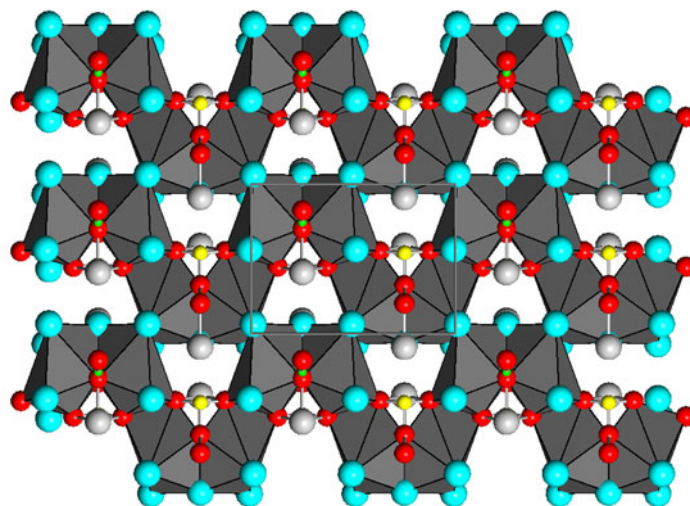


Figure 5. A layer of edge-sharing $[\text{Pb1O}_4\text{Cl}_4]$ polyhedra (dark grey) in guanyuanite parallel to (100). Light grey, aqua, red, yellow, and green spheres represent Pb, Cl, O, Se and H atoms, respectively. The unit cell is outlined. Drawn using *XtalDraw* software (Downs and Hall-Wallace, 2003).

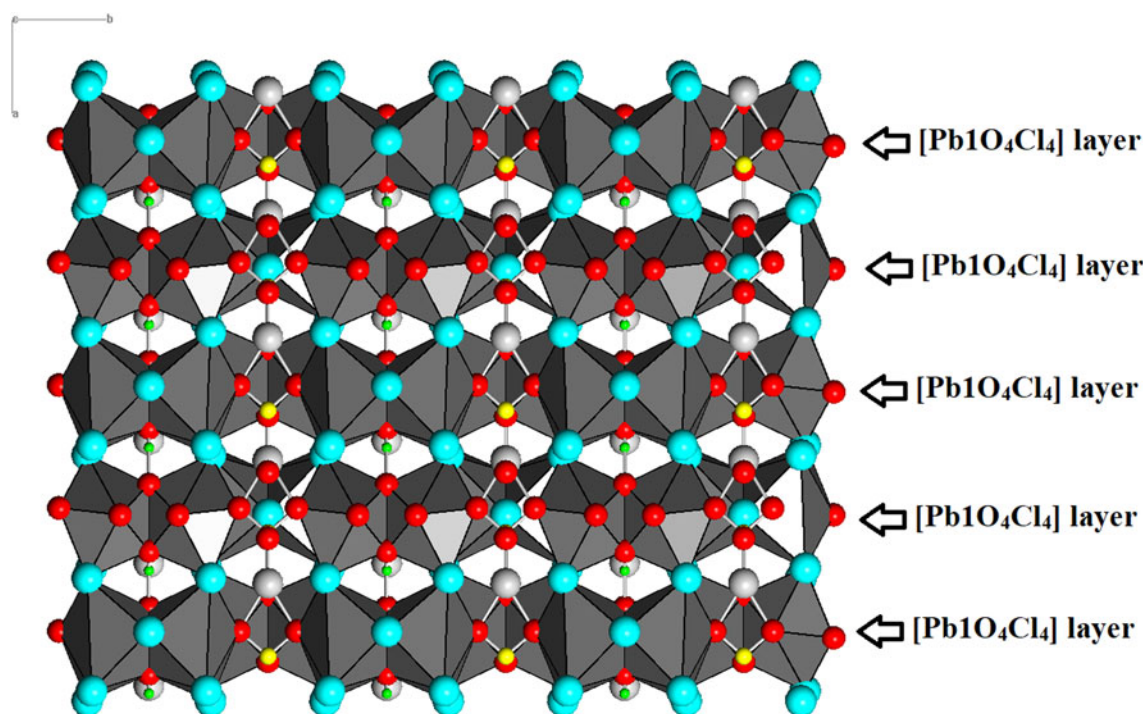


Figure 6. Crystal structure of guanyuanite, showing the stacking of layers of edge-sharing $[\text{Pb1O}_4\text{Cl}_4]$ polyhedra (dark grey) along the a -axis. The legends are the same as in Fig. 5.

with O2, with the O3...O2 distance of 2.707 Å (Table 7). According to the correlation between $\nu_{\text{O-H}}$ and O—H...O distances for minerals (Libowitzky, 1999), the Raman band centred at 3130 cm^{-1} corresponds well with the O...O distances between 2.70 and 2.80 Å. In comparison, the O—H stretching band is centred at 3201 cm^{-1} for isostructural $\text{Pb}_3\text{Br}_3(\text{Se}^{4+}\text{O}_3)(\text{OH})$ (Shang and Halasyamani, 2020), which has an O—H...O distance of 2.842 Å (Table 7). Because of similarities in both chemistry and structure between guanyuanite and orlandiite, $\text{Pb}_3\text{Cl}_4(\text{Se}^{4+}\text{O}_3)\cdot\text{H}_2\text{O}$ (Table 4), the Raman spectrum of orlandiite from the RRUFF Project (<http://rruff.info/R100122>) is also plotted in Fig. 3 for comparison. Evidently, the spectra of two minerals are very alike below 1000 cm^{-1} .

Guanyuanite is one of six lead selenite chloride minerals documented thus far (Table 1), after allochalcocelite $\text{Cu}^{1+}\text{Cu}_5^{2+}\cdot\text{PbO}^2(\text{SeO}_3)_2\text{Cl}_5$, orlandiite $\text{Pb}_3\text{Cl}_4(\text{Se}^{4+}\text{O}_3)\cdot\text{H}_2\text{O}$, prewittite $\text{KPb}_{1.5}\text{ZnCu}_6\text{O}_2(\text{SeO}_3)_2\text{Cl}_{10}$, sarrabusite $\text{Pb}_5\text{CuCl}_4(\text{SeO}_3)_4$ and wangkuirenite $\text{Pb}_3\text{Cl}_2(\text{Se}^{4+}\text{O}_3)_2$. Chemically, guanyuanite is very similar to orlandiite, the only hydrated mineral in this group. Interestingly, Porter *et al.* (2001) synthesised two lead selenite chlorides: $\text{Pb}_3\text{Cl}_3(\text{SeO}_3)(\text{SeO}_2\text{OH})$ and $\text{Pb}_3\text{Cl}_2(\text{SeO}_3)_2$, both of which are pseudo-layered, consisting of sheets of lead oxychloride polyhedra linked to $(\text{Se}^{4+}\text{O}_3)^{2-}$. The latter has been discovered recently in Nature as wangkuirenite (Yang *et al.*, 2023a), whereas the former has a chemical formula similar to that of guanyuanite. In fact, guanyuanite may be obtained from this compound

by removing the Se^{4+}O_2 molecule. As both $\text{Pb}_3\text{Cl}_3(\text{SeO}_3)$ (SeO_2OH) and $\text{Pb}_3\text{Cl}_2(\text{SeO}_3)_2$ (wangkuirenite) can be readily synthesised using a low-temperature (160°C) aqueous method (Porter *et al.*, 2001), the former compound may be found in Nature as well someday.

Acknowledgements. We are grateful for the constructive comments by Dr. Luca Bindi, Dr. Peter Leverett, and an anonymous reviewer. This study was funded by the Feinglos family and Mr. Michael M. Scott.

Supplementary material. The supplementary material for this article can be found at <https://doi.org/10.1180/mgm.2023.93>.

Competing interests. The authors declare none.

References

- Becker R., Johnsson M., Kremer R.K., Klauss H.H. and Lemmens P. (2006) Crystal structure and magnetic properties of $\text{FeTe}_2\text{O}_5\text{X}$ (X= Cl, Br): A frustrated spin cluster compound with a new Te(IV) coordination polyhedron. *Journal of the American Chemical Society*, **128**, 15469–15475.
- Becker R., Prester M., Berger H., Lin P.H., Johnsson M., Drobac D. and Zivkovic I. (2007) Crystal structure and magnetic properties of two new cobalt selenite halides: $\text{Co}_5(\text{SeO}_3)_4\text{X}_2$ (X= Cl, Br). *Journal of Solid State Chemistry*, **180**, 1051–1059.
- Berdonov P.S., Stefanovitch S.Y. and Dolgikh V.A. (2000) A new bismuth-selenium oxychloride, BiSeO_3Cl : crystal structure and dielectric and non-linear optical properties. *Journal of Solid State Chemistry*, **149**, 236–241.
- Berdonov P.S., Olenev A.V. and Dolgikh V.A. (2012) Lead (II) selenite halides $\text{Pb}_3(\text{SeO}_3)_2\text{X}_2$ (X= Br, I): Synthesis and crystal structure. *Crystallography Reports*, **57**, 200–204.
- Brown I.D. (2009) Recent developments in the methods and applications of the bond valence model. *Chemical Reviews*, **109**, 6858–6919.
- Cooper M.A. and Hawthorne F.C. (1995) Diaboleite, $\text{Pb}_2\text{Cu}(\text{OH})_4\text{Cl}_2$, a defect perovskite structure with stereoactive lone-pair behavior of Pb^{2+} . *The Canadian Mineralogist*, **33**, 1125–1129.
- Demartin F., Gramaccioli C.M. and Pilati T. (2003) The crystal structure of orlandiite, $\text{Pb}_3\text{Cl}_4(\text{SeO}_3)\cdot\text{H}_2\text{O}$, a complex case of twinning and disorder. *The Canadian Mineralogist*, **41**, 1147–1153.
- Dityat'yev O.A., Smidt P., Stefanovich S.Y., Lightfoot P., Dolgikh V.A. and Opperman H. (2004) Phase equilibria in the $\text{Bi}_2\text{TeO}_5\text{--Bi}_2\text{SeO}_5$ system and a high temperature neutron powder diffraction study of Bi_2SeO_5 . *Solid state sciences*, **6**, 915–922.
- Djemel M., Abdelhedi M., Ktari L. and Dammak M. (2013) X-ray diffraction, Raman study and electrical properties of the new mixed compound $\text{Rb}_{1.7}\text{K}_{0.3}(\text{SO}_4)_{0.88}(\text{SeO}_4)_{0.12}\text{Te}(\text{OH})_6$. *Journal of Molecular Structure*, **1047**, 15–21.
- Downs R.T. and Hall-Wallace M. (2003) The American mineralogist crystal structure database. *American Mineralogist*, **88**, 247–250.
- Finney J.J., Graeber E.J., Rosenzweig A. and Hamilton R.D. (1977) The structure of chloroxiphite, $\text{Pb}_3\text{CuO}_2(\text{OH})_2\text{Cl}_2$. *Mineralogical Magazine*, **41**, 357–361.
- Förster H.-J., Bindi L. and Stanley C.J. (2016) Grundmannite, CuBiSe_2 , the Se-analogue of emplectite, a new mineral from the El Dragón mine, Potosí, Bolivia. *European Journal of Mineralogy*, **28**, 467–477.
- Förster H.-J., Bindi L., Stanley C.J. and Grundmann G. (2017) Hansblockite, $(\text{Cu,Hg})(\text{Bi,Pb})\text{Se}_2$, the monoclinic polymorph of grundmannite: a new mineral from the Se mineralization at El Dragón (Bolivia). *Mineralogical Magazine*, **81**, 229–240.
- Förster H.-J., Bindi L., Grundmann G. and Stanley C.J. (2018) Cerramojonite, CuPbBiSe_3 , from El Dragón (Bolivia): A new member of the bournonite group. *Minerals*, **8**, 420.
- Förster H.-J., Ma C., Grundmann G., Bindi L. and Stanley C.J. (2019) Nickelyttrrellite, CuNi_2Se_4 , a New Member of the Spinel Supergroup from El Dragón, Bolivia. *The Canadian Mineralogist*, **57**, 637–646.
- Frost R.L. and Keeffe E.C. (2008) Raman spectroscopic study of the schmiederite $\text{Pb}_2\text{Cu}_2[(\text{OH})_4]\text{SeO}_3[\text{SeO}_4]$. *Journal of Raman Spectroscopy*, **39**, 1408–1402.
- Frost R.L., Weier M.L., Reddy B.J. and Cejka J. (2006) A Raman spectroscopic study of the uranyl selenite mineral haysenite. *Journal of Raman Spectroscopy*, **37**, 816–821.
- Gemmi M., Camprostrini I., Demartin F., Gorelik T.E. and Gramaccioli C.M. (2012) Structure of the new mineral sarrabusite, $\text{Pb}_5\text{CuCl}_4(\text{SeO}_3)_4$, solved by manual electron-diffraction tomography. *Acta Crystallographica*, **B68**, 15–23.
- Gillberg M. (1960) Perite, a new oxyhalide mineral from Långban, Sweden. *Arkiv för Mineralogi och Geologi*, **2**, 565–570.
- Giuseppetti G. and Tadini C. (1973) Riesame della struttura cristallina della nadorite: PbSbO_2Cl . *Periodico di Mineralogia*, **42**, 335–345.
- Gong Y.P., Hu C.L., Ma Y.X., Mao J.G. and Kong F. (2019) $\text{Pb}_2\text{Cd}(\text{SeO}_3)_2\text{X}_2$ (X= Cl and Br): two halogenated selenites with phase matchable second harmonic generation. *Inorganic Chemistry Frontiers*, **6**, 3133–3139.
- Grundmann G. and Förster H.-J. (2017) Origin of the El Dragón Selenium Mineralization, Quijarro Province, Potosí, Bolivia. *Minerals*, **7**, 1–68.
- Grundmann G., Lehrberger G. and Schnorrer-Köhler G. (1990) The El Dragón mine, Potosí, Bolivia. *Mineralogical Record*, **21**, 133–150.
- Grundmann G., Lehrberger G. and Schnorrer-Köhler G. (2007) The “El Dragón Mine”, Porco, Potosí, Bolivia – Selenium minerals. *Mineral UP*, **1**, 16–25.
- Holland T.J.B. and Redfern S.A.T. (1997) Unit cell refinement from powder diffraction data: the use of regression diagnostics. *Mineralogical Magazine*, **61**, 65–77.
- Jiang H.L. and Mao J.G. (2006) New members in the $\text{Ni}^{n+1}(\text{QO}_3)_n\text{X}_2$ family: unusual 3D network based on Ni_4ClO_3 cubane-like clusters in $\text{Ni}_7(\text{TeO}_3)_6\text{Cl}_2$. *Inorganic chemistry*, **45**, 7593–7599.
- Johnsson M., Törnroos K.W., Mila F. and Millet P. (2000) Tetrahedral clusters of copper(II): crystal structures and magnetic properties of $\text{Cu}_2\text{Te}_2\text{O}_5\text{X}_2$ (X= Cl, Br). *Chemistry of materials*, **12**, 2853–2857.
- Johnsson M., Törnroos K.W., Lemmens P. and Millet P. (2003) Crystal structure and magnetic properties of a new two-dimensional S= 1 quantum spin system $\text{Ni}_5(\text{TeO}_3)_4\text{X}_2$ (X= Cl, Br). *Chemistry of materials*, **15**, 68–73.
- Kampf A.R., Mills S.J. and Nash B.P. (2016a) Pauladamsite, $\text{Cu}_4(\text{SeO}_3)(\text{SO}_4)(\text{OH})_4\cdot 2\text{H}_2\text{O}$, a new mineral from the Santa Rosa mine, Darwin district, California, USA. *Mineralogical Magazine*, **80**, 949–958.
- Kampf A.R., Mills S.J., Nash B.P., Thorne B. and Favreau G. (2016b) Alfredopetrovite, a new selenite mineral from the El Dragón mine, Bolivia. *European Journal of Mineralogy*, **28**, 479–484.
- Kasatkin A.V., Plášil J., Marty J., Agakhanov A.A., Belakovskiy D.I. and Lykova I.S. (2014) Nestolaite, $\text{CaSeO}_3\cdot\text{H}_2\text{O}$, a new mineral from the Little Eva mine, Grand County, Utah, USA. *Mineralogical Magazine*, **78**, 497–505.
- Kim S.H., Yeon J. and Halasyamani P.S. (2009) Noncentrosymmetric polar oxide material, Pb_3SeO_5 : synthesis, characterization, electronic structure calculations, and structure–property relationships. *Chemistry of Materials*, **21**, 5335–5342.
- Kim M.K., Kim S.H., Chang H.Y., Halasyamani P.S. and Ok K.M. (2010) New noncentrosymmetric tellurite phosphate material: synthesis, characterization, and calculations of $\text{Te}_2\text{O}(\text{PO}_4)_2$. *Inorganic chemistry*, **49**, 7028–7034.
- Kong F., Huang S.P., Sun Z.M., Mao J.G. and Cheng W.D. (2006) $\text{Se}_2(\text{B}_2\text{O}_7)$: a new type of second-order NLO material. *Journal of the American Chemical Society*, **128**, 7750–7751.
- Kovrugin V.M., Colmont M., Siidra O.I., Mentré O., Al-Shuray A., Gurzhiy V.V. and Krivovichev S.V. (2015) Oxocentered Cu (ii) lead selenite honeycomb lattices hosting Cu (i) Cl₂ groups obtained by chemical vapor transport reactions. *Chemical Communications*, **51**, 9563–9566.
- Krivovichev S.V., Avdontseva E.Y. and Burns P.C. (2004) Synthesis and crystal structure of $\text{Pb}_3\text{O}_2(\text{SeO}_3)$. *Zeitschrift für anorganische und allgemeine Chemie*, **630**, 558–562.
- Lafuente B., Downs R.T., Yang H. and Stone N. (2015) The power of databases: the RRUFF project. Pp. 1–30 in: *Highlights in Mineralogical Crystallography* (T. Armbruster and R.M. Danisi, editors). W. De Gruyter, Berlin, Germany.
- Libowitzky E. (1999) Correlation of O–H stretching frequencies and O–H...O hydrogen bond lengths in minerals. *Monatshfte für Chemie*, **130**, 1047–1059.
- Mandarino J.A. (1981) The Gladstone–Dale relationship. IV. The compatibility concept and its application. *The Canadian Mineralogist*, **19**, 441–450.
- Millet P., Johnsson M., Pashchenko V., Ksari Y., Stepanov A. and Mila F. (2001) New copper (II)–lone electron pair elements–oxyhalides

- compounds: syntheses, crystal structures, and magnetic properties. *Solid State Ionics*, **141**, 559–565.
- Mills S.J., Kampf A.R., Housley R.M., Christy A.G., Thorne B., Chen Y.-S. and Steele I.M. (2014) Favreauite, a new selenite mineral from the El Dragón mine, Bolivia. *European Journal of Mineralogy*, **26**, 771–781.
- Ok K.M. and Halasyamani P.S. (2002) Anionic templating: Synthesis, structure, and characterization of novel three-dimensional mixed-metal oxychlorides $\text{Te}_4\text{M}_3\text{O}_{15}\text{Cl}$ ($\text{M} = \text{Nb}^{5+}$ or Ta^{5+}). *Inorganic Chemistry*, **41**, 3805–3807.
- Ok K.M., Bhuvanesh N.S.P. and Halasyamani P.S. (2001) Bi_2TeO_5 : synthesis, structure, and powder second harmonic generation properties. *Inorganic Chemistry*, **40**, 1978–1980.
- Paar W.H., Cooper M.A., Moëlo Y., Stanley C.J., Putz H., Topa D., Roberts A.C., Stirling J., Raith J.G. and Rowe R. (2012) Eldragónite, $\text{Cu}_6\text{BiSe}_4(\text{Se}_2)$, A new mineral species from the El Dragón Mine, Potosí, Bolivia, and its crystal structure. *The Canadian Mineralogist*, **50**, 281–294.
- Porter Y. and Halasyamani P.S. (2001) A low temperature method for the synthesis of new lead selenite chlorides: $\text{Pb}_3(\text{SeO}_3)(\text{SeO}_2\text{OH})\text{Cl}_3$ and $\text{Pb}_3(\text{SeO}_3)_2\text{Cl}_2$. *Inorganic Chemistry*, **40**, 2640–2641.
- Porter Y., Ok K.M., Bhuvanesh N.S.P. and Halasyamani P.S. (2001) Synthesis and characterization of Te_2SeO_7 : a powder second-harmonic-generating study of TeO_2 , Te_2SeO_7 , Te_2O_5 , and TeSeO_4 . *Chemistry of materials*, **13**, 1910–1915.
- Rouse R.C. (1973) Hematophanite, a derivative of the perovskite structure. *Mineralogical Magazine*, **39**, 49–53.
- Shang M. and Halasyamani P.S. (2020) Mixed lone-pair and mixed anion compounds: $\text{Pb}_3(\text{SeO}_3)(\text{HSeO}_3)\text{Br}_3$, $\text{Pb}_3(\text{SeO}_3)(\text{OH})\text{Br}_3$, $\text{CdPb}_8(\text{SeO}_3)_4\text{Cl}_4\text{Br}_6$ and $\text{RbBi}(\text{SeO}_3)\text{F}_2$. *Journal of Solid State Chemistry*, **282**, 121121.
- Sheldrick G.M. (2015a) SHELXT – Integrated space-group and crystal structure determination. *Acta Crystallographica*, **A71**, 3–8.
- Sheldrick G.M. (2015b) Crystal structure refinement with SHELX. *Acta Crystallographica*, **C71**, 3–8.
- Shuvalov R.R., Vergasova L.P., Semenova T.F., Filatov S.K., Krivovichev S.V., Siidra O.I. and Rudashevsky N.S. (2013) Prewittite, $\text{KPb}_{1.5}\text{Cu}_6\text{Zn}(\text{SeO}_3)_2\text{O}_2\text{Cl}_{10}$, a new mineral from Tolbachik fumaroles, Kamchatka peninsula, Russia: description and crystal structure. *American Mineralogist*, **98**, 463–469.
- Siidra O.I., Krivovichev S.V., Turner R.W. and Rumsey M.S. (2008) Chloroxiphite $\text{Pb}_3\text{CuO}_2(\text{OH})_2\text{Cl}_2$: structure refinement and description in terms of oxocentred OPb_4 tetrahedra. *Mineralogical Magazine*, **72**, 793–798.
- Siidra O., Kozin M.S., Depmeier W., Kayukov R.A. and Kovrugin V.M. (2018) Copper–lead selenite bromides: a new large family of compounds partly having Cu^{2+} substructures derivable from kagome nets. *Acta Crystallographica*, **B74**, 712–724.
- Vergasova L.P., Krivovichev S.V., Britvin S.N., Fitatov S.K., Berns P.K. and Ananyev V.V. (2005) Allochalcoselite, $\text{Cu}^+\text{Cu}_5^{2+}\text{PbO}_2(\text{SeO}_3)_2\text{Cl}_5$ – a new mineral from volcanic exhalations (Kamchatka, Russia). *Zapiski Rossiiskogo Mineralogicheskogo Obshchestva*, **134**, 70–74.
- Wickleder M.S. (2002) Inorganic lanthanide compounds with complex anions. *Chemical Reviews*, **102**, 2011–2088.
- Wickleder M.S., Buchner O., Wickleder C., Sheik S.E., Brunklaus G. and Eckert H. (2004) $\text{Au}_2(\text{SeO}_3)_2(\text{SeO}_4)$: Synthesis and characterization of a new noncentrosymmetric selenite-selenate. *Inorganic Chemistry*, **43**, 5860–5864.
- Yang H., McGlasson J.A., Ronald B. Gibbs R.B. and Downs R.T. (2022) Franksousaite, $\text{PbCu}(\text{Se}^{6+}\text{O}_4)(\text{OH})_2$, the Se^{6+} analogue of linarite, a new mineral from the El Dragón mine, Potosí, Bolivia. *Mineralogical Magazine*, **86**, 792–798.
- Yang H., Gu X., Gibbs R.B. and Downs R.T. (2023a) wangkuirenite, IMA 2023-030. CNMNC Newsletter 74. *Mineralogical Magazine*, **87**, 783–787, <https://doi.org/10.1180/mgm.2023.54>.
- Yang H., Gu X., Jenkins R.A., Gibbs R.B. and Downs R.T. (2023b) Bernardevansite, $\text{Al}_2(\text{Se}^{4+}\text{O}_3)_3 \cdot 6\text{H}_2\text{O}$, dimorphous with alfredopetrovite and the Al-analogue of mandarinoite, from the El Dragón mine, Potosí, Bolivia. *Mineralogical Magazine*, **87**, 1–8.
- Yang H., Gu X., Jenkins R.A., Gibbs R.B., McGlasson J.A. and Scott M.M. (2023c) Petermegawite, $\text{Al}_6(\text{Se}^{4+}\text{O}_3)_3[\text{SiO}_3(\text{OH})](\text{OH})_9 \cdot 10\text{H}_2\text{O}$, a new Al-bearing selenite mineral, from the El Dragón mine, Potosí, Bolivia. *The Canadian Journal of Mineralogy and Petrology*, **61**, 987–998.
- Yang, H., Gu, X., McGlasson, J.A. and Gibbs, R.B. (2023d) Guangyuanite, IMA 2022-124. CNMNC Newsletter 72; *Mineralogical Magazine*, **87**, <https://doi.org/10.1180/mgm.2023.21>
- Zhang D., Johnsson M., Berger H., Kremer R.K., Wulferding D. and Lemmens P. (2009) Separation of the oxide and halide part in the oxohalide $\text{Fe}_3\text{Te}_3\text{O}_{10}\text{Cl}$ due to high Lewis acidity of the cations. *Inorganic Chemistry*, **48**, 6599–6603.
- Zhang D., Berger H., Kremer R.K., Wulferding D., Lemmens P. and Johnsson M. (2010) Synthesis, crystal structure, and magnetic properties of the copper selenite chloride $\text{Cu}_5(\text{SeO}_3)_4\text{Cl}_2$. *Inorganic chemistry*, **49**, 9683–9688.
- Zhang S., Hu C., Li P., Jiang H. and Jiang-Gao Mao J. (2012) Syntheses, crystal structures and properties of new lead(II) or bismuth(III) selenites and tellurite. *Dalton Transactions*, **41**, 9532–9542.